CrossMark

ORIGINAL ARTICLE

Clinicopathologic implications of CD8$^+$/Foxp3$^+$ ratio and miR-574-3p/PD-L1 axis in spinal chordoma patients

Ming-Xiang Zou[1] · Ke-Miao Guo[1] · Guo-Hua Lv[1] · Wei Huang[2] · Jing Li[1] · Xiao-Bin Wang[1] · Yi Jiang[3] · Xiao-Ling She[3]

Abstract Currently, little is known about the interactions between microRNAs (miRNAs) and the PD-1/PD-L1 signaling pathway in chordoma, and data discussing the role of the immune milieu in chordoma prognosis are limited. We aimed to analyze the relationship between PD-L1, miR-574-3p, microenvironmental tumor-infiltrating lymphocytes (TILs) and clinicopathological features of spinal chordoma patients. PD-L1 expression and TILs (including Foxp3$^+$, CD8$^+$, PD-1$^+$ and PD-L1$^+$) were assessed by immunohistochemistry in tumor specimens of 54 spinal chordoma patients. MiRNAs microarray and bioinformatical analysis were used to identify miRNAs potentially regulating PD-L1 expression, which were further validated by quantitative RT-PCR. miR-574-3p was identified to potentially regulate PD-L1 expression in chordoma, which inversely correlated with PD-L1. Positive PD-L1 expression on tumor cells was associated with advanced stages ($P = 0.041$) and TILs infiltration ($P = 0.005$), whereas decreased miR-574-3p level correlated with higher muscle invasion ($P = 0.012$), more severe tumor necrosis ($P = 0.022$) and poor patient survival. Importantly, a patient subgroup with PD-L1$^+$/miR-574-3p^{low} chordoma phenotype was significantly associated with worse local recurrence-free survival (LRFS) ($P = 0.026$). PD-1$^+$ TILs density was associated with surrounding muscle invasion ($P = 0.014$), and independently portended poor LRFS ($P = 0.040$), while PD-L1$^+$ TILs showed tendencies of less aggressive clinical outcomes. Multivariate analysis of OS only found CD8$^+$/Foxp3$^+$ ratio to be independent prognostic factor ($P = 0.022$). These findings may be useful to stratify patients into prognostic groups and provide a rationale for the use of checkpoint blockade therapy, possibly by administering miR-574-3p mimics, in spinal chordoma.

Keywords Spinal chordoma · CD8 · Foxp3 · PD-1 · PD-L1 · miR-574-3p

List of abbreviations

FFPE	Formalin-fixed paraffin-embedded
Foxp3	Forkhead box P3
LRFS	Local relapse-free survival
miRNA	microRNA
qRT-PCR	quantitative RT-PCR
TILs	Tumor-infiltrating lymphocytes

✉ Jing Li
jingli1969@126.com

✉ Xiao-Bin Wang
wxbspine@hotmail.com

1 Department of Spine Surgery, The Second Xiangya Hospital, Central South University, 139 Renminzhong Road, Changsha, Hunan 410011, China

2 Institute of Precision Medicine, Xiangya Hospital, Central South University, Changsha 410008, China

3 Department of Pathology, The Second Xiangya Hospital, Central South University, Changsha 410011, China

Introduction

Being considered to arise from remnants of the embryonic notochord, chordoma is a very rare and slow-growing malignant mesenchymal neoplasm [1–3]. Clinically, chordoma accounts for 1–4% of all bone malignancies and has an age-adjusted incidence rate of less than one case per million [4–6]. As chordoma usually responds poorly to conventional chemotherapy and radiation treatment [3, 7], the cornerstone

of treatment for chordoma at present is complete surgical resection, which has been suggested to be the most important factor influencing chordoma recurrence and long-term patient survival [2, 7–9]. However, many patients will still have tumor recurrence after surgery and 5–40% of patients may even develop metastases [8, 10], which poses a big challenge in efficient clinical treatment and predicting the clinical course of the disease. Currently, despite significant advances in diagnosis, treatment modalities and the molecular understanding of chordoma, its prognosis still remains dismal. Thus, the development of novel chordoma-specific molecular targets is highly needed to improve therapeutic interventions and prognosis prediction for the patients.

The immune checkpoint of the PD-1/PD-L1 pathway is believed to represent a mechanism whereby cancer can evade host antitumor immune surveillance [11, 12]. Previous clinical trials have already shown promising results by PD-1/PD-L1-inhibitors in different cancer types [13]. The rationale of immune checkpoint blockade therapy is considered to directly activate T cells, especially CD8$^+$ cytotoxic tumor-infiltrating lymphocytes (CD8$^+$ TILs), in the tumor microenvironment [14–16]. Besides the above mechanism, previous studies also reported several available antibody-based drugs that could inhibit immunosuppressive Foxp3$^+$ regulatory T-lymphocyte (Foxp3$^+$ TILs) pathways [15]. As the major players in tumor immunity, CD8$^+$ TILs and Foxp3$^+$ TILs have been found to correlate with patient survival in many forms of human cancers [17, 18]. To date, expression patterns of the PD-1/PD-L1 axis and TILs has been described in the literature for chordoma [19, 20]. However, characterization of the different TIL subsets, especially CD8$^+$ TILs and Foxp3$^+$ TILs, in chordoma tumor lesions remains unknown.

MicroRNAs (miRNA) are a family of short endogenous non-coding RNA molecules that function to suppress protein coding gene expression through a complementary interaction with the 3′-UTR of target messenger RNAs [21, 22]. Previous studies have shown that miRNAs are implicated in chordoma development, growth, progression and prognosis [23, 24]. However, little is known about the interactions between miRNAs and the PD-1/PD-L1 signaling pathway in chordoma.

Currently, many studies have been conducted to investigate chordoma molecular biology and found several candidate prognostic biomarkers for risk stratification [25]. However, due to heterogeneity of tumor cells across chordoma, broad clinical application of such biomarkers has not been established yet. In recent years, the tumor immune microenvironment has been increasingly emphasized in pathological evaluation, which can offer meaningful and new information on prognosis. Furthermore, previous studies have demonstrated that the immune parameters within tumor regions have prognostic significance superior to that of traditional staging [26]. In this study, we aim to

discuss PD-L1 expression, microenvironmental TIL densities, (especially CD8$^+$ TILs and Foxp3$^+$ TIL levels as well as their ratio), in resected spinal chordoma and their association with clinicopathological features or outcome of spinal chordoma patients. We also attempt to identify miRNAs potentially regulating PD-L1 expression in spinal chordoma by miRNA microarray and bioinformatical analysis, and assess the impact of miRNAs/PD-L1 axis expression on patient survival.

Materials and methods

Patients and tissue samples

A total of 54 tumor tissue specimens from 54 spinal chordoma patients who were surgically treated at our Department between June 2002 and April 2015 were retrospectively collected. For a normal control, twenty nucleus pulposus tissue samples from 20 patients with disc herniation who underwent surgery during the same period were also retrieved. These two patient groups have previously been described in our study [27]. Patients who had received prior chemotherapy or radiotherapy and any other types of tumor-specific therapy were excluded for this study. Clinicopathological data, including age, gender, tumor size, location, tumor grade, stage, surrounding muscle invasion, preoperative recurrence, type of resection, tumor hemorrhage and necrosis, were retrospectively reviewed and obtained from patients' medical records (Supplementary Table 1). Tumor grade and stage were evaluated according to the Enneking staging system for the surgical staging of malignant bone and soft tissue tumors [2, 7, 28]. Resected tumor specimens were evaluated by anatomic pathologists and recorded as Enneking appropriate or Enneking inappropriate according to the Enneking principles [29]. The surrounding muscle invasion by chordoma was confirmed by preoperative magnetic resonance images and postoperative pathologic examination [30, 31]. Preoperative tumor recurrence was recorded in patients who had previously received tumor resection and had confirmed relapse on admission.

Immediately following surgery, tissue samples from both patient groups were immediately fixed in 10% buffered formalin and embedded in paraffin. The formalin-fixed paraffin-embedded (FFPE) blocks from tumor and normal tissues were retrieved from the Department of Pathology and processed into 4-μm thick sections. Chordoma diagnosis was made on histological examination of H&E-stained tumor tissue sections by two pathologists (Yi Jiang and Xiao-Ling She) according to the previously published criteria [3].

Follow-up

Patients were followed-up clinically and radiographically at three-month intervals in the first 2 years postoperatively, then every 6 months for 3 years after surgery, and annually thereafter. Diagnosis of local tumor recurrence was based on the clinical manifestations and imaging finding during follow-up or histology of the second surgery [1, 32]. Local relapse-free survival (LRFS) was defined as the time interval from the date of surgery to the diagnosis of the first local recurrence. Similarly, OS was defined as the interval between tumor resection and death from any causes. Observations were censored when the patient was tumor-free (LRFS analysis) or alive (OS analysis) until September 2015.

RNA isolation and miRNA microarray

Total RNA was extracted from 54 FFPE chordoma tissues and 20 FFPE nucleus pulposus samples using the mirVanaTM RNA isolation kit (Applied Biosystems, Frost city, CA, USA) following the manufacturer's instructions. The concentration of sample RNA was measured by a Nano-Drop 2000 spectrophotometer (Thermo Scientific, Waltham, MA, USA), and integrity was evaluated by agarose gel electrophoresis and ethidium bromide staining of 28 S and 18 S.

MiRNA microarray data were directly obtained from our prior studies and subject to the same analysis [33, 34]. Two-sided t tests and fold change were used to select differentially expressed miRNAs.

Bioinformatical analysis

We used the miRNA microarray data combined with three online complementary computational databases (miRanda, http://www.microrna.org/microrna/home.do; miRWalk2.0, http://zmf.umm.uni-heidelberg.de/apps/zmf/mirwalk2/; TargetScan, http://www.targetscan.org/) by the reverse algorithms to identify the potential miRNAs that might regulate expression of PD-L1 in spinal chordoma tissues. As previous studies consistently reported a positive or upregulated PD-L1 expression in various human-malignant tumors including chordoma [19, 20, 35–37], we only considered downregulated miRNAs from results of miRNA microarray as the candidate miRNAs.

Quantitative RT-PCR

Total RNA (10 ng) from tissue samples was reverse transcribed into cDNA using the miRNA Reverse Transcription Kit (Qiagen, Germany) according to the manufacturer's protocol. qPCR was conducted using a TaqMan® Universal PCR Master Mix (Applied Biosystems, CA). Melting curve

analysis was carried out to confirm the generation of specific amplified PCR products at the end of the PCR cycles. The relative miRNA expression levels were calculated using the $2^{-\Delta\Delta Ct}$ method [38], and U6 snRNA was used as an endogenous control. All experiments were performed in triplicate. The specific primers used in this study are shown in Supplementary Table 2.

Immunohistochemistry

Immunohistochemistry was performed using a peroxidase-labeled streptavidin–biotin technique as previously described [19, 27, 39]. Briefly, 4-µm thin sections were deparaffinized in xylene and rehydrated with graded ethanol solutions, and then exposed to antigen retrieval in pressure cooker at 127 °C for 15 min in EDTA buffer with pH 7.0. Then, tissue sections were incubated with 3% H_2O_2 in methanol for 15 min to quench potential endogenous peroxidase activity. Next, sections were incubated in 10% normal goat serum for 30 min at room temperature to block non-specific binding after three times washing in PBS. After this, sections were stained with primary anti-Foxp3 (clone 236A/E7, ab20034, Abcam, Cambridge, MA, USA) at a dilution of 1:20, anti-CD8 (bs-4790R, Bioss, Woburn, Massachusetts, USA) at a dilution of 1:100, anti-PD-1 (clone EPR4877(2), ab137132, Abcam) at a dilution of 1:400, anti-PD-L1 antibody (clone 28-8, ab205921, Abcam) at a dilution of 1:50 and anti-Ki-67 (clone SP6, ab16667, Abcam) at a dilution of 1:100 at 4 °C overnight. On the next day, tissue sections were washed with PBS and then incubated with a secondary biotinylated goat anti-rabbit immunoglobulin at 37 °C for 30 min, followed by a streptavidin–peroxidase conjugate (Auragene, Changsha, Hunan, China). Finally, 3,3′-diaminobenzidine solution was added to visualize antibody binding, counterstained lightly with hematoxylin. Negative controls were created by replacing the primary antibody with PBS, and positive control sections were from human-non-malignant lymph node tissues as previously suggested [19, 40].

Evaluation of immunohistochemical analysis

Semiquantitative analysis

Immunohistochemistry results were evaluated independently by two well-experienced pathologists (Yi Jiang and Xiao-Ling She) who were blinded for the presented clinical outcomes. The overall degree of TILs was assessed on full H&E sections using a semiquantitative evaluation criteria as previously described [19, 20, 41], and TILs were judged to be: absent (0), rare/few (1), moderate (2) or prominent (3). The tissue samples were then classified into negative if a score of 0–1 was observed (score 0–1) and positive if a score of 2–3 was otherwise demonstrated. The pattern of Foxp3+,

CD8^{+}, PD-1^{+} and PD-L1^{+} TILs were analyzed by the same scoring scale (0–3) and recorded as absent (0), rare/few (1), moderate (2) or prominent (3), similar to a previous report [41]. Ki-67 index in tumor tissues was recorded as percentage of cells with positive nuclear staining and these data were grouped into low (< 10% positivity) and high Ki-67 expression (≥ 10% positivity) according to the criteria proposed by Zhou et al. [31]. PD-L1 expression was defined as positive if ≥ 5% of tumor cells had membrane staining, as suggested by previous reports [19, 42, 43].

Automated image analysis

Automated image analysis of TILs was performed for slides stained for Foxp3, CD8, PD-1 and PD-L1 as previously described [44, 45]. Briefly, sections were viewed in areas where TIL density was focally high or representative of the TIL distribution as a whole using Nikon's inverted Eclipse Ti microscope and the images were acquired with Nikon DS-Ri 1-U3 digital camera (Tokyo, Japan. Camera control unit DS-U3) using NIS-Elements image analysis software AR 3.0. The enumeration of Foxp3^{+}, CD8^{+}, PD-1^{+} and PD-L1^{+} TILs was then performed in five hotspots (20×) using a computer-assisted image analysis method (Image-pro plus 6.0, Media Cybernetics, Inc., Rockville, MD, USA). Finally, the numbers of positively stained cells per unit area (mm^2) were calculated and the mean densities were obtained.

Statistical analysis

All statistical analyses were performed using SPSS 17.0 (SPSS, Chicago, IL, USA). The data were analyzed using Student's *t* test or One-Way ANOVA test for two continuous variables (presented as mean ± standard deviation) and Chi-square test or Wilcoxon's rank sum test for categorical variables, where appropriate. Pearson's correlation test was used to examine the relationship between two continuous variables. The threshold value for selecting differentially expressed miRNAs was placed at *P* value ≦ 0.05 with fold change ≧ 2 and False discovery rate < 0.05, which was calculated to correct the *P* value. Cutoff Finder Web Application (http://molpath.charite.de/cutoff) was used to determine the threshold value for prognosis analysis [46], which was defined as the point with the most significant split (smallest *P* value from the log-rank test). The Kaplan–Meier method was performed to estimate LRFS and OS curves, and the differences in survival probability were determined by univariate analysis using the log-rank test. Multivariate Cox proportional hazard models were used to identify independent factors significantly associated with LRFS and OS by including variables that were significant in univariate analysis. All

tests were two-sided and a *P* value ≤ 0.05 was considered statistically significant.

Results

Patient characteristics

54 patients with spinal chordoma who underwent curative resection at our institute were included. There were 35 males and 19 females, with a mean age of 55.59 ± 13.56 years (ranging between 23 and 79 years). 43 had primary spinal chordomas and 11 had recurrent diseases. All patients had conventional chordoma subtype and were followed-up until September 2015, with an average follow-up period of 42.39 months (range 5–158 months). Other patient characteristics are summarized in Supplementary Table 1.

Differentially expressed miRNAs in chordoma tissue samples

As per our previous selection criteria, 182 of 2006 human mature miRNAs were differentially expressed in chordoma compared with nucleus pulposus tissues (as controls). Among them, 110 was upregulated and 72 was downregulated (Supplementary Figure 1).

Identification of miR-574-3p as a potential regulator of PD-L1 expression in spinal chordoma

As shown in Supplementary Table 3 and Supplementary Figure 2, six downregulated miRNAs were found to potentially regulate PD-L1 expression. The quantitative RT-PCR results confirmed the findings from the miRNA microarray except for miR-371b-5p, which was found to have no significant difference in expression between chordoma and nucleus pulposus tissues (Supplementary Figure 3a). However, further analysis only showed a significant inverse association between miR-574-3p and PD-L1 (Supplementary Figure 3b).

Expression of miR-574-3p, PD-L1, microenvironmental TILs and their correlations with clinicopathologic features of chordoma patients

The expression level of miR-574-3p in chordoma tissues was significantly lower than that in nucleus pulposus samples (*t* = 8.463, *P* < 0.001, Supplementary Figure 3a). In addition, chordoma with reduced miR-574-3p expression was significantly associated with higher muscle invasion and more severe tumor necrosis (*t* = 2.612, *P* = 0.012 and *F* = 3.520, *P* = 0.022, respectively, Table 1). PD-L1 expression was positive in tumor cells in 37 of 54 patients (68.5%,

Table 1 Association between miR-574-3p/PD-L1 expression, microenvironmental TILs and clinicopathological features of spinal chordoma patients

Clinicopathological factors	PD-1+ TILs[a]			PD-L1+ TILs[a]			PD-L1 in tumor[b]			Tumor miR-574-3p expression[a]		
	No. of patients (n = 54)	Mean ± SD	P	No. of patients (n = 54)	Mean ± SD	P	Negative (n = 17)	Positive (n = 37)	P	No. of patients (n = 54)	Mean ± SD	P
Age (years)												
≤ 50	23	128.3 ± 128.1	0.224	23	315.6 ± 196.7	0.348	7	16	0.880	23	14.3 ± 7.6	0.401
> 50	31	169.2 ± 115.6		31	268.0 ± 171.7		10	21		31	12.6 ± 7.2	
Sex												
Male	35	170.8 ± 127.9	0.120	35	291.3 ± 151.0	0.871	12	23	0.540	35	13.5 ± 7.6	0.750
Female	19	116.8 ± 103.3		19	282.7 ± 234.5		5	14		19	12.9 ± 6.9	
Tumor size												
≤ 5 cm	21	175.4 ± 146.5	0.259	21	263.0 ± 153.6	0.422	6	15	0.710	21	12.5 ± 8.3	0.510
> 5 cm	33	136.8 ± 102.4		33	304.3 ± 199.4		11	22		33	13.8 ± 6.6	
Tumor location												
Sacral vertebra	42	137.1 ± 102.3	0.099	42	316.5 ± 185.0	**0.032**	14	28	0.840	42	14.0 ± 7.5	0.211
Cervical or thoracic or lumbar vertebra	12	203.0 ± 169.2		12	189.5 ± 138.8		3	9		12	11.0 ± 6.1	
Surrounding muscle invasion												
Yes	36	180.0 ± 125.8	**0.014**	36	269.7 ± 162.6	0.295	11	25	0.830	36	9.8 ± 7.3	**0.012**
No	18	95.3 ± 92.2		18	325.4 ± 217.4		6	12		18	15.1 ± 6.8	
Preoperative recurrence												
Yes	11	167.8 ± 143.9	0.629	11	325.4 ± 194.9	0.455	6	5	0.130	11	12.0 ± 9.1	0.498
No	43	147.7 ± 116.9		43	278.7 ± 180.4		11	32		43	13.7 ± 6.9	
Grade												
High	38	149.3 ± 124.2	0.819	38	184.9 ± 137.2	**0.006**	15	23	0.051	38	13.4 ± 7.4	0.943
Low	16	157.7 ± 119.0		16	331.7 ± 183.1		2	14		16	13.2 ± 7.4	
Stage												
IA	13	71.0 ± 65.8	0.678	13	418.5 ± 63.7	**0.035**	2	11	**0.041**	13	12.1 ± 7.1	0.674
IB	6	151.9 ± 133.2		6	419.8 ± 227.9		0	6		6	11.0 ± 6.0	
IIA	4	122.0 ± 88.6		4	315.5 ± 186.3		3	1		4	14.1 ± 9.5	
IIB	27	165.2 ± 125.2		27	205.8 ± 140.0		9	18		27	14.7 ± 7.7	
III	4	164.8 ± 135.4		4	169.7 ± 161.6		3	1		4	10.7 ± 6.2	
Type of resection												
EI	18	171.3 ± 119.2	0.407	18	292.1 ± 151.3	0.914	5	13	0.670	18	13.2 ± 7.4	0.873
EA	36	142.0 ± 123.3		36	286.3 ± 198.3		12	24		36	13.5 ± 7.3	
Tumor hemorrhage												
No	10	130.7 ± 117.1	0.549	10	266.1 ± 195.5	0.675	3	7	1.00	10	12.7 ± 6.7	0.762

Table 1 (continued)

Clinicopathological factors	PD-1+ TILs[a]			PD-L1+ TILs[a]			PD-L1 in tumor[b]			Tumor miR-574-3p expression[a]		
	No. of patients (n = 54)	Mean ± SD	P	No. of patients (n = 54)	Mean ± SD	P	Negative (n = 17)	Positive (n = 37)	P	No. of patients (n = 54)	Mean ± SD	P
Yes	44	156.6 ± 123.5		44	293.3 ± 181.5		14	30		44	13.5 ± 7.5	
Tumor necrosis												
Absent	13	137.8 ± 101.4	0.945	13	254.2 ± 157.2	0.407	4	9	0.410	13	19.2 ± 5.5	0.022
Mild	18	158.0 ± 145.0		18	250.3 ± 142.2		5	13		18	14.0 ± 9.0	
Moderate	15	147.4 ± 129.7		15	344.7 ± 225.1		3	12		15	13.3 ± 6.7	
Severe	8	168.8 ± 94.3		8	323.1 ± 212.9		5	3		8	9.6 ± 5.3	
Ki-67 index												
Low	25	144.8 ± 124.8	0.698	25	285.5 ± 200.0	0.920	8	17	0.930	25	14.2 ± 8.1	0.406
High	29	157.8 ± 120.7		29	290.6 ± 170.0		9	20		29	12.5 ± 6.6	

Clinicopathological factors	CD8+ TILs[a]			Foxp3+ TILs[a]			CD8+/Foxp3+ ratio[a]		
	No. of patients (n = 54)	Mean ± SD	P	No. of patients (n = 54)	Mean ± SD	P	No. of patients (n = 50)	Mean ± SD	P
Age (years)									
≤ 50	23	333.0 ± 283.6	0.623	23	121.0 ± 116.0	0.559	20	3.9 ± 3.4	0.269
> 50	31	295.4 ± 271.7		31	140.0 ± 115.5		30	2.9 ± 2.9	
Sex									
Male	35	334.6 ± 281.6	0.405	35	131.0 ± 117.3	0.950	32	3.5 ± 3.4	0.579
Female	19	268.6 ± 263.9		19	133.1 ± 113.8		18	2.9 ± 2.6	
Tumor size									
≤ 5 cm	21	343.6 ± 287.5	0.497	21	142.7 ± 125.0	0.579	18	3.2 ± 3.4	0.874
> 5 cm	33	290.9 ± 268.9		33	124.7 ± 109.6		32	3.3 ± 2.9	
Tumor location									
Sacral vertebra	42	306.7 ± 287.3	0.816	42	131.0 ± 121.7	0.938	40	3.4 ± 3.2	0.533
Cervical or thoracic or lumbar vertebra	12	327.9 ± 236.4		12	134.0 ± 92.3		10	2.7 ± 2.5	
Surrounding muscle invasion									
Yes	36	326.4 ± 299.3	0.574	36	131.2 ± 112.5	0.964	33	3.2 ± 3.3	0.779
No	18	327.9 ± 236.4		18	132.7 ± 123.2		17	3.5 ± 2.7	
Preoperative recurrence									
Yes	11	350.8 ± 341.2	0.599	11	163.7 ± 129.8	0.305	10	2.8 ± 3.7	0.593
No	43	301.3 ± 259.0		43	123.5 ± 111.1		40	3.4 ± 3.0	

Table 1 (continued)

Clinicopathological factors	CD8+ TILs[a]			Foxp3+ TILs[a]			CD8+/Foxp3+ ratio[a]		
	No. of patients (n = 54)	Mean ± SD	P	No. of patients (n = 54)	Mean ± SD	P	No. of patients (n = 50)	Mean ± SD	P
Grade									
High	38	337.2 ± 278.8	0.293	38	127.6 ± 106.4	0.692	36	3.5 ± 3.3	0.473
Low	16	250.2 ± 263.5		16	141.4 ± 136.7		14	2.8 ± 2.7	
Stage									
IA	13	242.2 ± 230.3	0.451	13	152.5 ± 137.0	0.477	12	2.6 ± 2.8	0.512
IB	6	176.3 ± 157.3		6	117.0 ± 98.6		6	2.3 ± 2.2	
IIA	4	372.0 ± 412.5		4	160.3 ± 60.9		4	2.2 ± 2.0	
IIB	27	347.1 ± 287.7		27	109.3 ± 102.5		24	4.1 ± 3.6	
III	4	437.3 ± 313.9		4	208.8 ± 178.2		4	2.9 ± 1.8	
Type of resection									
EI	18	264.2 ± 290.6	0.378	18	120.8 ± 112.1	0.626	16	2.4 ± 2.1	0.190
EA	36	335.0 ± 267.6		36	137.2 ± 117.6		34	3.7 ± 3.4	
Tumor hemorrhage									
No	10	300.1 ± 261.0	0.887	10	157.9 ± 115.1	0.430	10	2.5 ± 3.0	0.384
Yes	44	314.0 ± 280.7		44	125.8 ± 115.5		40	3.5 ± 3.1	
Tumor necrosis									
Absent	13	400.0 ± 261.0	0.504	13	132.3 ± 83.8	0.995	13	4.4 ± 4.0	0.495
Mild	18	244.9 ± 242.2		18	132.7 ± 143.2		17	3.0 ± 3.0	
Moderate	15	312.2 ± 273.9		15	125.7 ± 108.2		13	2.8 ± 2.5	
Severe	8	315.6 ± 369.6		8	139.6 ± 121.0		7	2.6 ± 1.9	
Ki-67 index									
Low	25	364.0 ± 270.5	0.195	25	140.1 ± 111.6	0.624	25	3.7 ± 2.7	0.349
High	29	266.1 ± 275.0		29	124.5 ± 119.3		25	2.7 ± 3.4	

EI Enneking inappropriate, *EA* Enneking appropriate, *TILs* tumor-infiltrating lymphocytes, *PD-1* programmed cell death-1, *PD-L1* programmed cell death-1 ligand 1, *SD* standard deviation

[a] By Student's *t* test or one-way ANOVA test

[b] By Chi-square test or Wilcoxon's rank sum test

Fig. 1 Immunohistochemistry analysis of PD-L1 expression levels. **a** Positive expression of PD-L1 in chordoma tissues; **b** negative expression of PD-L1 in chordoma tissues; **c** positive expression of PD-L1 in nucleus pulposus tissues; **d** negative PD-L1 expression in nucleus pulposus tissues (× 400)
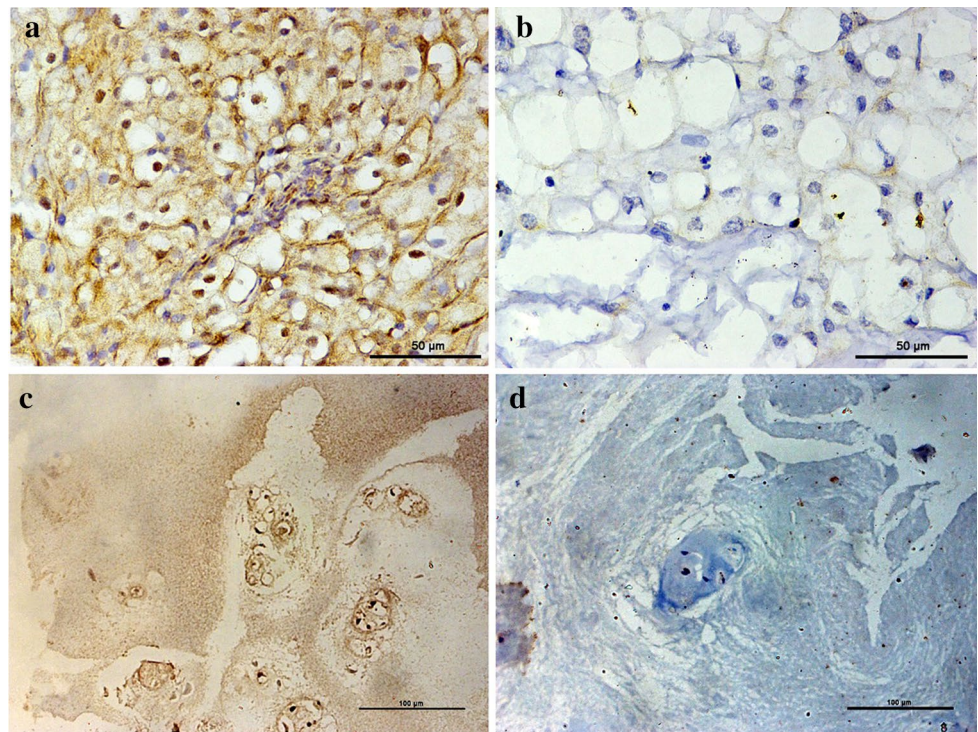

Fig. 1a, b). In contrast, PD-L1 was expressed in nucleus pulposus tissues in 5 of 20 cases (25.0%, Fig. 1c, d) and the difference was statistically significant ($\chi^2 = 11.260$, $P < 0.001$). We also found that patients with positive PD-L1 expression exhibited advanced stages at presentation ($Z = -2.039$, $P = 0.041$, Table 1).

Overall, TILs were present in all 54 patient samples after assessing the H&E sections. Specifically, the overall TIL level was scored as rarely or a few in 23 (42.6%), moderate in 15 (27.8%), and prominent in 16 (29.6%) cases (Supplementary Figure 4a–c). Therefore, the overall TIL expression was negative (0 or 1) in 23 (42.6%) and positive (2 or 3) in 31 (57.4%) cases. PD-1 and PD-L1 were expressed in TILs in all 54 samples (Supplementary Table 4 and Supplementary Figure 4d–i). The average intratumoral PD-1$^+$ and PD-L1$^+$ TILs densities were 151.8 cells/mm^2 and 288.0 cells/mm^2, respectively (Supplementary Table 1). Increased PD-1$^+$ TIL infiltration was associated with higher tumor invasion of the surrounding muscle tissue ($t = -2.531$, $P = 0.014$, Table 1). However, a low level of PD-L1+ TILs was correlated with higher pathological grade ($t = -2.878$, $P = 0.006$), advanced stages ($F = 2.815$, $P = 0.035$) and tumor location at the mobile spine ($t = 2.201$, $P = 0.032$) (Table 1). The pattern of CD8$^+$ or Foxp3$^+$ TILs in chordoma tissues fell into four categories (Supplementary Table 4 and Supplementary Figure 5a-h). The mean intratumoral CD8$^+$ or Foxp3$^+$ TILs density, and CD8$^+$/Foxp3$^+$ TILs ratio were 311.0 cells/mm^2, 132.0 cells/mm^2 and 3.3, respectively (Supplementary Table 1). However, there was no statistically

significant relationship found between CD8$^+$ or Foxp3$^+$ TILs density, or CD8$^+$/Foxp3$^+$ ratio and clinicopathological variables examined (Table 1).

Association between microenvironmental TILs and miR-574-3p/PD-L1 axis

Tumors with PD-L1-positive expression were more likely to have lymphocyte tumor infiltration (Supplementary Table 5). However, tumor miR-574-3p expression was found to have no significant correlation with TIL infiltration in chordoma microenvironment (Supplementary Figure 6f).

The mean PD-1$^+$ TIL densities were significantly higher in chordoma tissues with positive PD-L1 expression as compared with tissue harboring negative PD-L1 expression ($t = 2.718$, $P = 0.009$, Supplementary Figure 6a). However, chordomas with negative PD-L1 expression were tended to have more number of PD-L1$^+$ TILs in tumor microenvironment than those with positive PD-L1 expression ($t = 2.951$, $P = 0.005$, Supplementary Figure 6b). Similar observation was also found for CD8$^+$/Foxp3$^+$ ratio, which was lower in PD-L1-expressed tumors than the PD-L1-negative counterparts ($t = 2.764$, $P = 0.008$, Supplementary Figure 6c). However, Foxp3$^+$ TILs or CD8$^+$ TILs alone were not significantly associated with PD-L1 expression (Supplementary Figure 6d, e).

CD8$^+$/Foxp3$^+$ ratio was closely associated with miR-574-3p expression (Supplementary Figure 7a and Supplementary Table 5). We also observed a moderate correlation

between PD-1^{+} TIL and PD-L1^{+} TIL densities, and between CD8^{+} TIL and Foxp3^{+} TIL densities (Supplementary Table 5 and Supplementary Figure 7b, c). In addition, CD8^{+}/Foxp3^{+} ratio was correlated with the number of PD-1^{+} TILs, Foxp3^{+} TILs and CD8^{+} TILs (Supplementary Table 5 and Supplementary Figure 7d-f).

Influence of miR-574-3p and PD-L1 expression and TILs on spinal chordoma prognosis

During the follow-up period, 41 patients (75.93%) had local recurrence and 24 patients (44.44%) died. The estimated 1- and 3-year LRFS rates were 70.1% and 9.6%, while the estimated 1-, 3-, 5- and 10-year OS rates were 88.4, 51.6, 44.1 and 35.3%, respectively. Median LRFS and OS were

21.0 months (range 3–45 months) and 48.0 months (range 5–158 months), respectively.

The prognostic cut-offs in relation to LRFS and OS for miR-574-3p and TILs are listed in Supplementary Table 6. Patients were divided into high (≥ cutoff) or low expression group (< cutoff) according to the cutoff values. Kaplan–Meier analysis showed that high tumor miR-574-3p expression was statistically associated with better LRFS (Table 2 and Fig. 2a). In addition, coexpression of PD-L1 and miR-574-3p in tumor cells was significantly associated with LRFS (Table 2 and Fig. 2b). Subgroup analysis indicated that positive PD-L1 and low miR-574-3p expression levels were associated with much poorer survival when compared with positive PD-L1 and high miR-574-3p-expressed tumors (median, 12 vs.

Table 2 Univariate and multivariate Cox proportional hazard analyses of prognostic factors for local recurrence-free survival of spinal chordoma patients

Factors	Categories	Univariate analysis		Multivariate analysis (with CD8^{+}/Foxp3^{+} ratio)[a]		Multivariate analysis (with CD8^{+} TILs)[a]	
		χ^2	P value	P value	HR (95% CI)	P value	HR (95% CI)
Sex	Male/female	2.949	0.086				
Age	≤ 50/> 50	6.560	**0.010**	0.451	1.462 (0.545–3.917)	0.395	1.454 (0.614–3.441)
Tumor size	≤ 5 cm/> 5 cm	0.278	0.59				
Tumor location	Sacral vertebra/cervical or thoracic or lumbar vertebra	0.003	0.95				
Preoperative recurrence	Yes/no	0.954	0.32				
Surrounding muscle invasion	Yes/no	24.585	**< 0.001**	**0.009**	3.900 (1.400–10.863)	**0.009**	3.538 (1.376–9.097)
Grade	High/low	0.231	0.631				
Stage	IA/IB/IIA/IIB/III	0.960	0.916				
Type of resection	EI/EA	16.472	**< 0.001**	0.529	1.375 (0.509–3.715)	0.547	1.363 (0.498–3.732)
Tumor hemorrhage	Yes/no	4.031	**0.045**	0.125	2.446 (0.781–7.657)	0.082	2.701 (0.881–8.281)
Tumor necrosis	Absent/mild/moderate/severe	0.189	0.97				
Extent of overall TILs	Negative/positive	4.104	**0.043**	0.304	1.601 (0.652–3.929)	0.346	1.522 (0.635–3.649)
Ki-67 index	High/low	14.163	**< 0.001**	0.105	2.082 (0.857–5.056)	0.111	2.078 (0.845–5.111)
PD-L1 expression on tumor cells	Negative/positive	3.406	0.065				
Tumor miR-574-3p expression	High/low	6.350	**0.012**	0.269	0.613 (0.258–1.460)	0.293	0.635 (0.272–1.481)
PD-L1/miR-574-3p coexpression	Low/low	6.359	**0.042**	0.443	0.837 (0.532–1.318)	0.570	0.883 (0.575–1.356)
	High/low						
	Low/high						
	High/high						
PD-1[+] TILs	High/low	17.731	**< 0.001**	**0.040**	3.268 (1.053–10.138)	**0.040**	3.046 (1.053–8.806)
PD-L1^{+} TILs	High/low	10.789	**0.001**	0.446	0.590 (0.152–2.291)	0.316	0.510 (0.137–1.902)
CD8^{+} TILs	High/low	7.700	**0.006**			0.262	0.532 (0.177–1.602)
Foxp3^{+} TILs	High/low	0.661	0.416				
CD8^{+}/Foxp3^{+} ratio	High/low	7.696	**0.006**	0.098	0.412 (0.144–1.179)		

Bold values indicate $P < 0.05$

EI Enneking inappropriate, *EA* Enneking appropriate, *TILs* tumor-infiltrating lymphocytes, *PD-1* programmed cell death 1, *PD-L1* programmed cell death-1 ligand 1, *HR* hazard ratio, *CI* confidence interval

[a] CD8^{+}/Foxp3^{+} ratio and CD8^{+} TILs were not simultaneously included in the multivariate analysis because they are closely correlated and seem to be confounded with each other
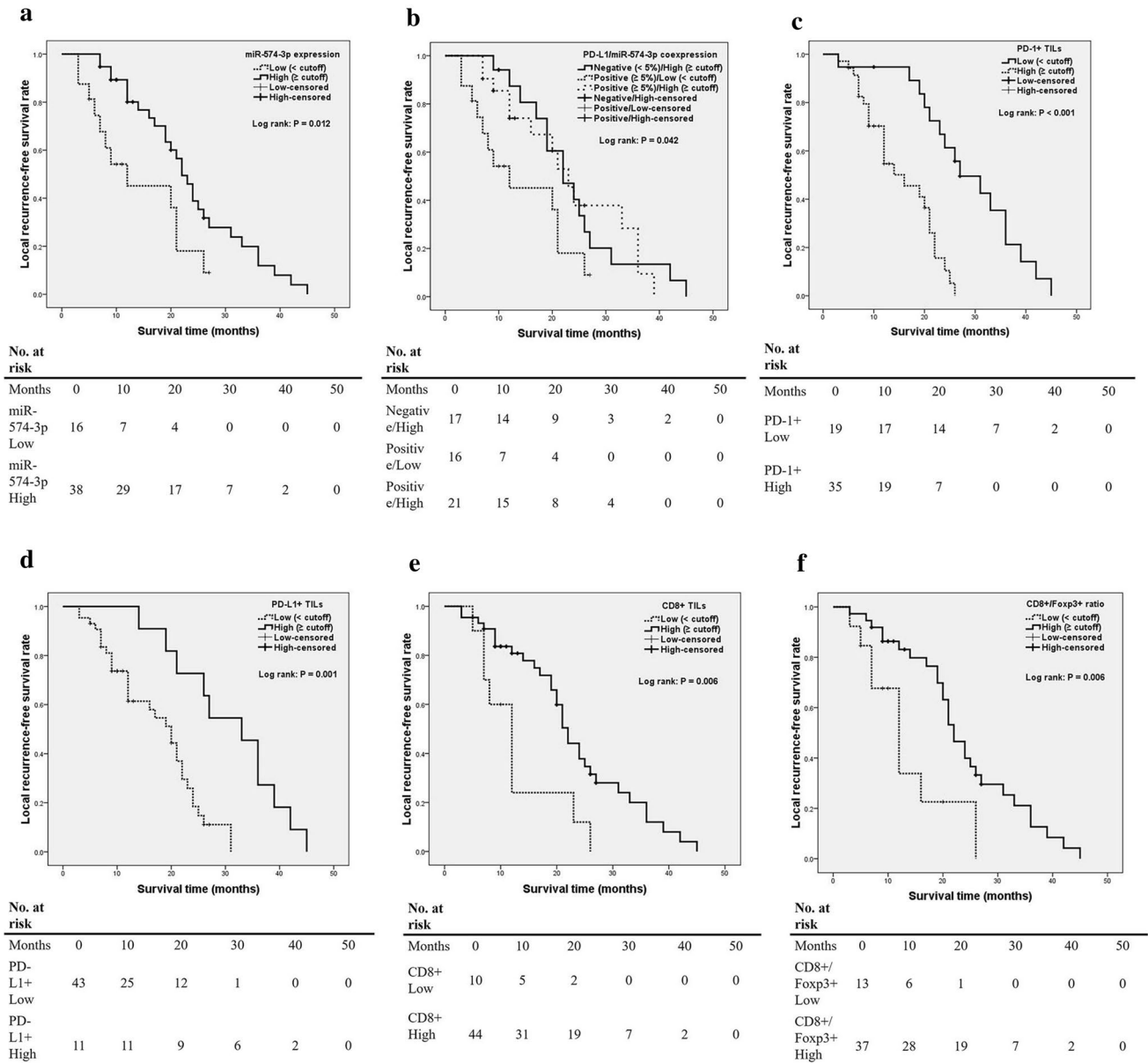
Fig. 2 Kaplan–Meier curves of the local recurrence-free survival of patients. **a** Stratified by miR-574-3p expression ($P = 0.012$ via log-rank test); **b** stratified by miR-574-3p/PD-L1 coexpression ($P = 0.042$); **c** stratified by PD-1^{+} TILs density ($P < 0.001$); **d** stratified by PD-L1^{+} TILs density ($p = 0.001$); **e** stratified by CD8^{+} TILs density ($P = 0.006$); **f** stratified by CD8^{+}/Foxp3^{+} ratio ($P = 0.006$)

23 months, $P = 0.026$; log-rank). Furthermore, we found that the levels of PD-1^{+} TILs, PD-L1^{+} TILs, CD8^{+} TILs as well as CD8^{+}/Foxp3^{+} ratio were statistically associated with LRFS (Table 2 and Fig. 2c–f). Multivariate analyses showed that PD-1 expression in TILs and surrounding muscle invasion by tumor were independent predictors for LRFS (Table 2). Moreover, CD8^{+}/Foxp3^{+} ratio tended to have more statistically powerful prognostic value on LRFS than CD8^{+} TILs alone, though such prognostic implication did not reach significance (Table 2).

Regarding OS, Kaplan–Meier analysis showed that high tumor miR-574-3p expression was statistically associated with better OS (Table 3 and Fig. 3a). Similar associations were also observed between OS and high CD8^{+}/Foxp3^{+} ratio or PD-L1^{+} TILs density (Table 3 and Fig. 3b, c). However, patients with high PD-1^{+} TIL or Foxp3^{+} TIL density experienced worse OS (Table 3 and Fig. 3d, e). In addition, coexpression of PD-L1 and miR-574-3p in tumor cells was significantly associated with OS (Table 3). However, we found no significant difference in survival outcome between

Table 3 Univariate and multivariate Cox proportional hazard analyses of prognostic factors for overall survival of spinal chordoma patients

Factors	Categories	Univariate analysis		Multivariate analysis (with CD8+/Foxp3+ ratio)[a]		Multivariate analysis (with Foxp3+ TILs)[a]	
		χ^2	P value	P value	HR (95% CI)	P value	HR (95% CI)
Sex	Male/female	1.540	0.21				
Age	$\leq 50/> 50$	1.459	0.22				
Tumor size	≤ 5 cm/> 5 cm	0.127	0.72				
Tumor location	Sacral vertebra/cervical or thoracic or lumbar vertebra	0.132	0.71				
Preoperative recurrence	Yes/no	0.546	0.46				
Surrounding muscle invasion	No/yes	6.793	**0.009**	0.732	0.806 (0.235–2.761)	0.847	1.121 (0.352–3.571)
Grade	High/low	0.641	0.42				
Stage	IA/IB/IIA/IIB/III	22.303	**< 0.001**	0.054	1.569 (0.993–2.480)	0.344	1.214 (0.813–1.813)
Type of resection	EI/EA	5.898	**0.015**	0.132	2.152 (0.795–5.828)	0.245	1.827 (0.662–5.043)
Tumor hemorrhage	Yes/no	0.319	0.57				
Tumor necrosis	Absent/mild/moderate/severe	4.032	0.25				
Extent of overall TILs	Negative/positive	0.003	0.95				
Ki-67 index	High/low	2.045	0.15				
PD-L1 expression on tumor cells	Negative/positive	1.047	0.30				
Tumor miR-574-3p expression	High/low	10.863	**0.001**	0.965	0.167 (0.002–13.945)	0.966	0.171 (0.002–14.621)
PD-L1/miR-574-3p coexpression	Low/low	14.699	**0.002**	0.168	0.709 (0.435–1.156)	0.226	0.750 (0.470–1.195)
	High/low						
	Low/high						
	High/high						
PD-1+ TILs	High/low	7.842	**0.005**	0.743	1.301 (0.271–6.248)	0.195	2.487 (0.627–9.864)
PD-L1+ TILs	High/low	6.868	**0.009**	0.138	0.209 (0.026–1.657)	0.837	0.834 (0.147–4.727)
CD8+ TILs	High/low	1.041	0.308				
Foxp3+ TILs	High/low	5.083	**0.024**			0.123	2.158 (0.811–5.743)
CD8+/Foxp3+ ratio	High/low	9.116	**0.003**	**0.022**	0.153 (0.031–0.761)		

Bold values indicate $P < 0.05$

EI Enneking inappropriate, *EA* Enneking appropriate, *TILs* tumor-infiltrating lymphocytes, *PD*-1 programmed cell death 1, *PD-L1* programmed cell death-1 ligand 1, *HR* hazard ratio, *CI* confidence interval

[a] CD8+/Foxp3+ ratio and Foxp3+ TILs were not simultaneously included in the multivariate analysis because they are closely correlated and seem to be confounded with each other

patients with PD-L1⁻/miR-574-3p^low and PD-L1⁺/miR-574-3p^low chordoma phenotype ($\chi^2 = 0.782$, $P = 0.376$ by the log-rank test). Multivariate Cox proportional hazards model showed CD8+/Foxp3+ ratio was significantly associated with the risk of death (Table 3). However, when Foxp3+ TILs instead of CD8+/Foxp3+ ratio was included in the analysis, no parameters were found to be independently predictive of OS (Table 3).

Discussion

In the current study, we assessed the profile of PD-L1 expression and recruited TILs as well as their clinicopathologic implication in spinal chordoma. We also attempted to determine miRNAs potentially regulating the PD-L1 expression in spinal chordoma using microarray and bioinformatical analysis and its influence on patient outcome. We observed an inverse correlation between PD-L1 and miR-574-3p, suggesting its potential regulatory function in PD-L1 expression. Tumor PD-L1 expression was significantly associated with TIL infiltration and advanced chordoma stage, while miR-574-3p expression was related to higher tumor muscle invasion, more severe tumor necrosis and increased CD8+/Foxp3+ ratio. Moreover, a patient subgroup with both negative PD-L1 and high miR-574-3p expression was found to have improved survival and reduced recurrence. For tumor microenvironment with respect to TILs, we found
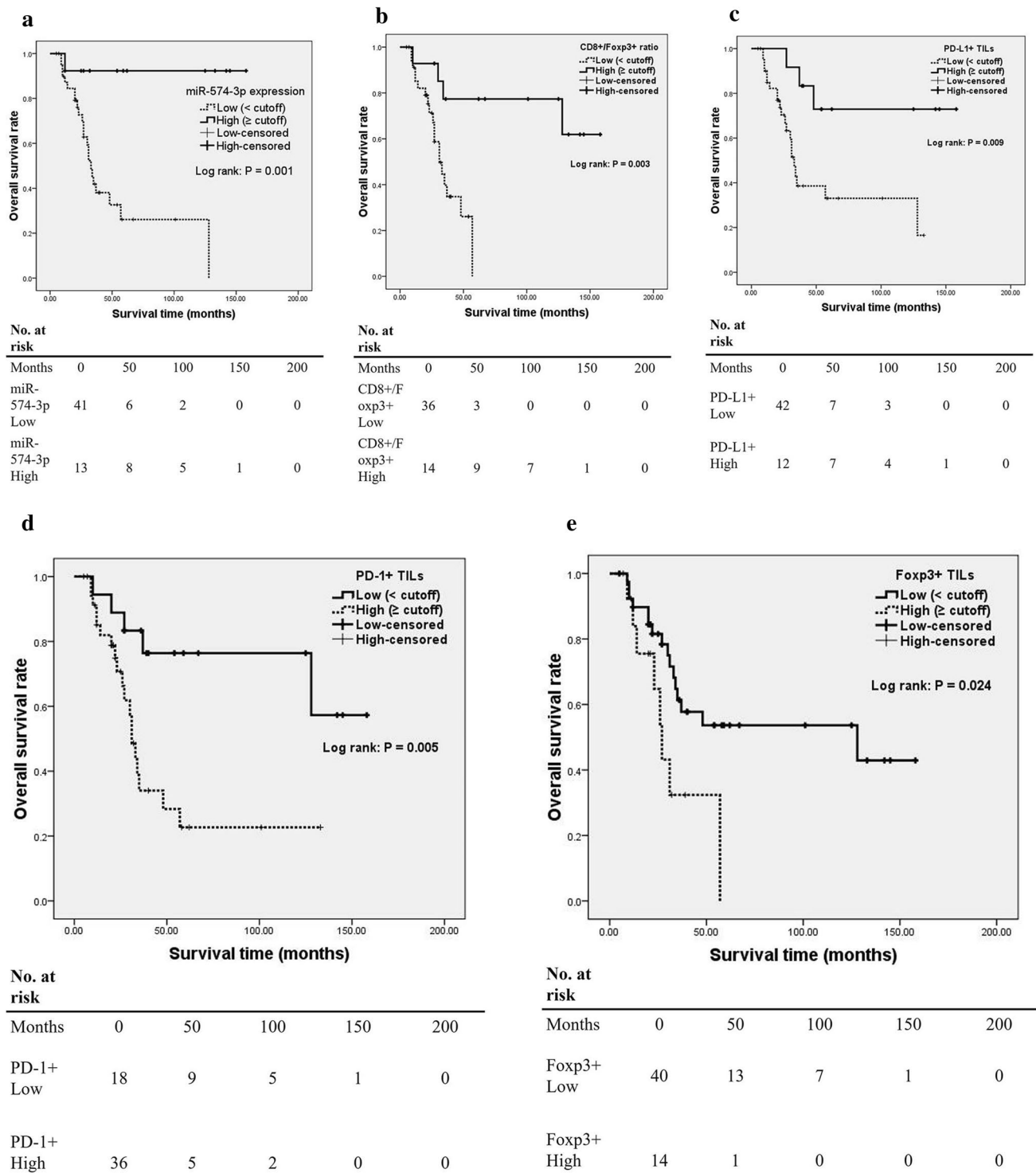
a

No. at risk					
Months	0	50	100	150	200
miR-574-3p Low	41	6	2	0	0
miR-574-3p High	13	8	5	1	0

b

No. at risk					
Months	0	50	100	150	200
CD8+/Foxp3+ Low	36	3	0	0	0
CD8+/Foxp3+ High	14	9	7	1	0

c

No. at risk					
Months	0	50	100	150	200
PD-L1+ Low	42	7	3	0	0
PD-L1+ High	12	7	4	1	0

d

No. at risk					
Months	0	50	100	150	200
PD-1+ Low	18	9	5	1	0
PD-1+ High	36	5	2	0	0

e

No. at risk					
Months	0	50	100	150	200
Foxp3+ Low	40	13	7	1	0
Foxp3+ High	14	1	0	0	0

Fig. 3 Kaplan–Meier curves of the overall survival of spinal chordoma patients. **a** Stratified by miR-574-3p ($P = 0.001$ via log-rank test); **b** stratified by CD8^{+}/Foxp3^{+} ratio ($P = 0.003$); **c** stratified by PD-L1^{+} TILs density ($P = 0.009$); **d** stratified by PD-1^{+} TILs density ($P = 0.005$) and **e** stratified by Foxp3^{+} TILs density ($P = 0.024$)

that TILs were frequently present in chordoma tissues and these immune cells distributed in a related manner. All TIL subtypes studied as well as CD8^{+}/Foxp3^{+} ratio were significantly associated with LRFS or/and OS. Moreover, high level of PD-1-positive lymphocyte infiltration was independently associated with poor LRFS. Importantly, CD8^{+}/

Foxp3$^+$ ratio was an independent predictor for OS. These findings may be useful to stratify patients into prognostic groups and provide a rationale for the use of checkpoint blockade therapy possibly by targeting miR-574-3p in spinal chordoma.

Recently, antibody blockade of the PD-1/PD-L1 axis has shown promising efficacy against several advanced human cancers [13]. Preliminary findings indicate that clinical responses to immune checkpoint inhibitors are associated with elevated PD-L1 expression on tumor cells [47, 48]. Therefore, assessing the profile of tumoral PD-L1 expression is essential to select patients who are likely to benefit from the immune checkpoint therapy. In this study, we found that PD-L1 was expressed in most chordoma specimens (68.5%), consistent with previous reports of PD-L1 immunopositivity in most human solid tumor samples including chordoma [19, 20, 36, 37]. Currently, the precise molecular mechanisms by which PD-L1 is upregulated in chordoma remain elusive. Previous studies demonstrated that hypoxia-inducible factor-1α was frequently expressed in chordoma tissues [49–51]. It will be interesting to postulate that PD-L1 upregulation in chordoma may be induced by the hypoxia conditions [52, 53]. In addition, it has been reported that upregulation of PD-L1 can be induced in response to exogenous inflammatory signals or driven by constitutive oncogenic signaling pathways [54]. Our study showed no significant association between PD-L1 and CD8$^+$ TILs, suggesting that the tumor-intrinsic pathways might be predominant mechanisms underlying PD-L1 overexpression in chordoma.

In this study, we used miRNA microarray and bioinformatical analysis to identify upstream differentially expressed miRNAs that may be involved in the regulation of PD-L1 expression in chordoma. We found that miR-574-3p was significantly downregulated in chordoma tumor samples as compared with corresponding nucleus pulposus tissues. Furthermore, a significant negative correlation between miR-574-3p and PD-L1 expression was observed, which suggests a potential regulatory role of miR-574-3p in PD-L1 expression. Previous data indicated that miR-574-3p might be a tumor suppressor in some human cancers [55–58] and was also correlated with higher Gleason score as well as advanced tumor stage in prostate cancer specimens [57]. Our study offers the first evidence that the reduced miR-574-3p expression is associated with poor clinicopathological features and survival outcomes of spinal chordoma patients. Furthermore, we also showed that chordoma harboring positive PD-L1 expression correlated with advanced stages. More importantly, the combined low miR-574-3p and high PD-L1 expression levels separated patients with worse survival outcome from those with prolonged survival. Taken together, these results indicate that the downregulating of miR-574-3p expression in chordoma may exert its oncogenic function by targeting the PD-1/PD-L1 pathway, thereby promoting the proliferation and invasion of chordoma cells due to the tumor immune escape. Targeting PD-L1, possibly by the administration of miR-574-3p mimics, might be a potential therapeutic strategy in chordoma, similar to a previous report [59].

Many biomarkers have been reported in association with spinal chordoma prognosis [25]. However, due to the potential intertumoral and intratumoral heterogeneity, there are still no reliable molecular markers to predict clinical outcome and drug treatment response of chordoma. Previous studies showed that analysis of the tumor immune microenvironment might be less affected by tumor heterogeneity [60]. Additionally, it has been suggested that pathological immunity evaluation can provide more powerful information on prognosis, which may add to the significance of traditional staging [26]. In the present study, we focused on the spinal chordoma tumor microenvironment with respect to CD8$^+$ TILs and Foxp3$^+$ TILs. We found that the patient subgroup with high intratumoral CD8$^+$/Foxp3$^+$ TILs ratio had both improved LRFS and OS. Consistent with our findings, several studies made good prognostic claims for this ratio in esophageal squamous cell cancer, aggressive breast cancer and osteosarcoma [39, 60, 61]. Furthermore, in line with our study, it has also been determined that the CD8$^+$/Foxp3$^+$ TILs ratio was a more effective indicator than CD8$^+$ or Foxp3$^+$ TILs alone in esophageal cancer prognosis [39]. These findings indicate that a reciprocal interaction exists between CD8$^+$ TILs and Foxp3$^+$ TILs in human cancers including chordoma [39, 62].

Interestingly, we also found that intratumoral infiltration of PD-1$^+$ TILs independently predicted poor survival in spinal chordoma. This result is in agreement with previous studies showing negative prognostic implication for tumor-infiltrating PD-1-positive lymphocytes in soft-tissue sarcomas and clear cell renal cell carcinoma [63, 64]. Nevertheless, our analyses failed to show significant association between patient survival and infiltration of PD-L1-positive T cells, which contradicts our previous report and recent results from a meta-analysis [19, 65]. This inconsistency may be attributed to different definition and methodology used when assessing the PD-L1$^+$ TILs, as well as the different sets of prognostic factors included in the multivariate analysis.

To confirm our findings, additional prospective studies with large sample sizes are needed to validate our current data. Our study is a correlation study that lacks target gene function validation and cell-function experiments. Further studies are needed to demonstrate the complete miR-574-3p-mediated PD-L1 signaling networks in spinal chordoma and determine how their expressions influence the clinical outcome of patients. It should also be noted that use of the minimum P value method may lead to overestimation of the true effects on survival. We used this

approach to dichotomize continuous predictors because it enables us to stratify patients and then make recommendations for clinical management, and because of its wide use in prognosis studies [66–68]. Besides, we did not separately analyze TILs in different subareas in the tumor microenvironment, such as cancer stroma, invasive margin or cancer cell nests. Finally, some other kinds of immune cells within the tumor microenvironment, such as CD3^{+}, CD4^{+}, CD57^{+}, CD68^{+} and CD66b^{+} cells [69], may also be evaluated to enable more accurate understanding of the immune microenvironment parameters and their prognostic role in spinal chordoma.

Conclusions

This study identified miR-574-3p as a potential regulator of PD-L1 expression in chordoma. The expression of miR-574-3p/PD-L1 axis was significantly associated with clinicopathologic and immune characteristics of spinal chordoma patients. CD8^{+}/Foxp3^{+} ratio and the number of TIL subsets showed significant prognostic effects on patients' outcome. These findings may be useful to stratify patients into prognostic groups and provide a rationale for the use of checkpoint blockade therapy possibly by targeting miR-574-3p in spinal chordoma. However, further studies are still required to determine the complete miRNA-mediated PD-L1 signaling networks, and to evaluate whether the immune component of the tumor microenvironment could be effective predictive markers in spinal chordoma.

References

1. Hu H, Yang HL, Lu J, Chen KW, Qiu YH, Liu W, Luo ZP (2012) Association of telomerase expression with recurrence of sacral chordoma. Ann Oncol 23(10):2772
2. Samson IR, Springfield DS, Suit HD, Mankin HJ (1993) Operative treatment of sacrococcygeal chordoma. A review of twenty-one cases. J Bone Joint Surg Am 75(10):1476–1484
3. Walcott BP, Nahed BV, Mohyeldin A, Coumans JV, Kahle KT, Ferreira MJ (2012) Chordoma: current concepts, management, and future directions. Lancet Oncol 13(2):e69–e76
4. Bompas E, Le Cesne A, Tresch-Bruneel E, Lebellec L, Laurence V, Collard O, Saada-Bouzid E, Isambert N, Blay JY, Amela EY, Salas S, Chevreau C, Bertucci F, Italiano A, Clisant S, Penel N (2015) Sorafenib in patients with locally advanced and metastatic chordomas: a phase II trial of the French Sarcoma Group (GSF/GETO). Ann Oncol 26(10):2168–2173
5. McMaster ML, Goldstein AM, Bromley CM, Ishibe N, Parry DM (2001) Chordoma: incidence and survival patterns in the United States, 1973–1995. Cancer Causes Control 12(1):1–11
6. Bydon M, Papadimitriou K, Witham T, Wolinsky JP, Bydon A, Sciubba D, Gokaslan Z (2012) Novel therapeutic targets in chordoma. Expert Opin Ther Targets 16(11):1139–1143
7. Kayani B, Hanna SA, Sewell MD, Saifuddin A, Molloy S, Briggs TW (2014) A review of the surgical management of sacral chordoma. Eur J Surg Oncol 40(11):1412–1420
8. Fuchs B, Dickey ID, Yaszemski MJ, Inwards CY, Sim FH (2005) Operative management of sacral chordoma. J Bone Joint Surg Am 87(10):2211–2216
9. Kayani B, Sewell MD, Tan KA, Hanna SA, Williams R, Pollock R, Skinner J, Briggs TW (2015) Prognostic factors in the operative management of sacral chordomas. World Neurosurg 84(5):1354–1361
10. Baratti D, Gronchi A, Pennacchioli E, Lozza L, Colecchia M, Fiore M, Santinami M (2003) Chordoma: natural history and results in 28 patients treated at a single institution. Ann Surg Oncol 10(3):291–296
11. Dong H, Strome SE, Salomao DR, Tamura H, Hirano F, Flies DB, Roche PC, Lu J, Zhu G, Tamada K, Lennon VA, Celis E, Chen L (2002) Tumor-associated B7-H1 promotes T-cell apoptosis: a potential mechanism of immune evasion. Nat Med 8(8):793–800
12. Iwai Y, Ishida M, Tanaka Y, Okazaki T, Honjo T, Minato N (2002) Involvement of PD-L1 on tumor cells in the escape from host immune system and tumor immunotherapy by PD-L1 blockade. Proc Natl Acad Sci USA 99(19):12293–12297
13. Marcq E, Pauwels P, van Meerbeeck JP, Smits EL (2015) Targeting immune checkpoints: new opportunity for mesothelioma treatment? Cancer Treat Rev 41(10):914–924
14. Senbabaoglu Y, Gejman RS, Winer AG, Liu M, Van Allen EM, de Velasco G, Miao D, Ostrovnaya I, Drill E, Luna A, Weinhold N, Lee W, Manley BJ, Khalil DN, Kaffenberger SD, Chen Y, Danilova L, Voss MH, Coleman JA, Russo P, Reuter VE, Chan TA, Cheng EH, Scheinberg DA, Li MO, Choueiri TK, Hsieh JJ, Sander C, Hakimi AA (2016) Tumor immune microenvironment characterization in clear cell renal cell carcinoma identifies prognostic and immunotherapeutically relevant messenger RNA signatures. Genome Biol 17(1):231
15. Gajewski TF, Schreiber H, Fu YX (2013) Innate and adaptive immune cells in the tumor microenvironment. Nat Immunol 14(10):1014–1022
16. Rizvi NA, Hellmann MD, Snyder A, Kvistborg P, Makarov V, Havel JJ, Lee W, Yuan J, Wong P, Ho TS, Miller ML, Rekhtman N, Moreira AL, Ibrahim F, Bruggeman C, Gasmi B, Zappasodi R, Maeda Y, Sander C, Garon EB, Merghoub T, Wolchok JD, Schumacher TN, Chan TA (2015) Cancer immunology. Mutational

landscape determines sensitivity to PD-1 blockade in non-small cell lung cancer. Science 348(6230):124–128

17. Gooden MJ, de Bock GH, Leffers N, Daemen T, Nijman HW (2011) The prognostic influence of tumour-infiltrating lymphocytes in cancer: a systematic review with meta-analysis. Br J Cancer 105(1):93–103

18. deLeeuw RJ, Kost SE, Kakal JA, Nelson BH (2012) The prognostic value of FoxP3+ tumor-infiltrating lymphocytes in cancer: a critical review of the literature. Clin Cancer Res 18(11):3022–3029

19. Zou MX, Peng AB, Lv GH, Wang XB, Li J, She XL, Jiang Y (2016) Expression of programmed death-1 ligand (PD-L1) in tumor-infiltrating lymphocytes is associated with favorable spinal chordoma prognosis. Am J Transl Res 8(7):3274–3287

20. Feng Y, Shen J, Gao Y, Liao Y, Cote G, Choy E, Chebib I, Mankin H, Hornicek F, Duan Z (2015) Expression of programmed cell death ligand 1 (PD-L1) and prevalence of tumor-infiltrating lymphocytes (TILs) in chordoma. Oncotarget 6(13):11139–11149

21. Bartel DP (2004) MicroRNAs: genomics, biogenesis, mechanism, and function. Cell 116(2):281–297

22. Inui M, Martello G, Piccolo S (2010) MicroRNA control of signal transduction. Nat Rev Mol Cell Biol 11(4):252–263

23. Yu X, Li Z (2015) Epigenetic deregulations in chordoma. Cell Prolif 48(5):497–502

24. Gulluoglu S, Tuysuz EC, Kuskucu A, Ture U, Atalay B, Sahin F, Bayrak OF (2016) The potential function of microRNA in chordomas. Gene 585(1):76–83

25. Zou MX, Lv GH, Wang XB, Li J (2016) Prognostic biomarkers in spinal chordoma: a systematic review. J Neuropathol Exp Neurol 75(12):1184–1187

26. Galon J, Pages F, Marincola FM, Angell HK, Thurin M, Lugli A, Zlobec I, Berger A, Bifulco C, Botti G, Tatangelo F, Britten CM, Kreiter S, Chouchane L, Delrio P, Arndt H, Asslaber M, Maio M, Masucci GV, Mihm M, Vidal-Vanaclocha F, Allison JP, Gnjatic S, Hakansson L, Huber C, Singh-Jasuja H, Ottensmeier C, Zwierzina H, Laghi L, Grizzi F, Ohashi PS, Shaw PA, Clarke BA, Wouters BG, Kawakami Y, Hazama S, Okuno K, Wang E, O'Donnell-Tormey J, Lagorce C, Pawelec G, Nishimura MI, Hawkins R, Lapointe R, Lundqvist A, Khleif SN, Ogino S, Gibbs P, Waring P, Sato N, Torigoe T, Itoh K, Patel PS, Shukla SN, Palmqvist R, Nagtegaal ID, Wang Y, D'Arrigo C, Kopetz S, Sinicrope FA, Trinchieri G, Gajewski TF, Ascierto PA, Fox BA (2012) Cancer classification using the Immunoscore: a worldwide task force. J Transl Med 10:205

27. Zou MX, Lv GH, Li J, She XL, Jiang Y (2016) Upregulated human telomerase reverse transcriptase (hTERT) expression is associated with spinal chordoma growth, invasion and poor prognosis. Am J Transl Res 8(2):516–529

28. Jemal A, Siegel R, Ward E, Murray T, Xu J, Thun MJ (2007) Cancer statistics. CA Cancer J Clin 57(1):43–66

29. Fisher CG, Saravanja DD, Dvorak MF, Rampersaud YR, Clarkson PW, Hurlbert J, Fox R, Zhang H, Lewis S, Riaz S, Ferguson PC, Boyd MC (2011) Surgical management of primary bone tumors of the spine: validation of an approach to enhance cure and reduce local recurrence. Spine (Phila Pa 1976) 36(10):830–836

30. Chen K, Mo J, Zhou M, Wang G, Wu G, Chen H, Zhang K, Yang H (2014) Expression of PTEN and mTOR in sacral chordoma and association with poor prognosis. Med Oncol 31(4):886

31. Zhou M, Chen K, Yang H, Wang G, Lu J, Ji Y, Wu C, Chen C (2014) Expression of insulin-like growth factor II mRNA-binding protein 3 (IMP3) in sacral chordoma. J Neurooncol 116(1):77–82

32. Meng T, Yin H, Li B, Li Z, Xu W, Zhou W, Cheng M, Wang J, Zhou L, Yang X, Liu T, Yan W, Song D, Xiao J (2015) Clinical features and prognostic factors of patients with chordoma in the spine: a retrospective analysis of 153 patients in a single center. Neuro Oncol 17(5):725–732

33. Zou MX, Huang W, Wang XB, Li J, Lv GH, Wang B, Deng YW (2015) Reduced expression of miRNA-1237-3p associated with poor survival of spinal chordoma patients. Eur Spine J 24(8):1738–1746

34. Zou MX, Huang W, Wang XB, Lv GH, Li J, Deng YW (2014) Identification of miR-140-3p as a marker associated with poor prognosis in spinal chordoma. Int J Clin Exp Pathol 7(8):4877–4885

35. Wang A, Wang HY, Liu Y, Zhao MC, Zhang HJ, Lu ZY, Fang YC, Chen XF, Liu GT (2015) The prognostic value of PD-L1 expression for non-small cell lung cancer patients: a meta-analysis. Eur J Surg Oncol 41(4):450–456

36. Zhang Y, Kang S, Shen J, He J, Jiang L, Wang W, Guo Z, Peng G, Chen G, He J, Liang W (2015) Prognostic significance of programmed cell death 1 (PD-1) or PD-1 ligand 1 (PD-L1) expression in epithelial-originated cancer: a meta-analysis. Medicine (Baltimore) 94(6):e515

37. Wu P, Wu D, Li L, Chai Y, Huang J (2015) PD-L1 and survival in solid tumors: a meta-analysis. PLoS One 10(6):e0131403

38. Livak KJ, Schmittgen TD (2001) Analysis of relative gene expression data using real-time quantitative PCR and the 2(-Delta Delta C(T)) method. Methods 25(4):402–408

39. Zhu Y, Li M, Mu D, Kong L, Zhang J, Zhao F, Li Z, Liu X, Bo C, Yu J (2016) CD8+/FOXP3+ ratio and PD-L1 expression associated with survival in pT3N0M0 stage esophageal squamous cell cancer. Oncotarget 7(44):71455–71465

40. Berghoff AS, Fuchs E, Ricken G, Mlecnik B, Bindea G, Spanberger T, Hackl M, Widhalm G, Dieckmann K, Prayer D, Bilocq A, Heinzl H, Zielinski C, Bartsch R, Birner P, Galon J, Preusser M (2016) Density of tumor-infiltrating lymphocytes correlates with extent of brain edema and overall survival time in patients with brain metastases. Oncoimmunology 5(1):e1057388

41. Bellmunt J, Mullane SA, Werner L, Fay AP, Callea M, Leow JJ, Taplin ME, Choueiri TK, Hodi FS, Freeman GJ, Signoretti S (2015) Association of PD-L1 expression on tumor-infiltrating mononuclear cells and overall survival in patients with urothelial carcinoma. Ann Oncol 26(4):812–817

42. Teng F, Meng X, Wang X, Yuan J, Liu S, Mu D, Zhu H, Kong L, Yu J (2016) Expressions of CD8+ TILs, PD-L1 and Foxp3+ TILs in stage I NSCLC guiding adjuvant chemotherapy decisions. Oncotarget 7(39):64318–64329

43. Kollmann D, Ignatova D, Jedamzik J, Chang YT, Jomrich G, Paireder M, Kristo I, Kazakov D, Michal M, Cozzio A, Hoetzenecker W, Schatton T, Asari R, Preusser M, Guenova E, Schoppmann SF (2017) Expression of programmed cell death protein 1 by tumor-infiltrating lymphocytes and tumor cells is associated with advanced tumor stage in patients with Esophageal Adenocarcinoma. Ann Surg Oncol 24(9):2698–2706

44. Li S, Xu F, Li H, Zhang J, Zhong A, Huang B, Lai M (2017) S100A8+ stroma cells predict a good prognosis and inhibit aggressiveness in colorectal carcinoma. Oncoimmunology 6(1):e1260213

45. Gabrielson A, Wu Y, Wang H, Jiang J, Kallakury B, Gatalica Z, Reddy S, Kleiner D, Fishbein T, Johnson L, Island E, Satoskar R, Banovac F, Jha R, Kachhela J, Feng P, Zhang T, Tesfaye A, Prins P, Loffredo C, Marshall J, Weiner L, Atkins M, He AR (2016) Intratumoral CD3 and CD8 T-cell densities associated with relapse-free survival in HCC. Cancer Immunol Res 4(5):419–430

46. Budczies J, Klauschen F, Sinn BV, Gyorffy B, Schmitt WD, Darb-Esfahani S, Denkert C (2012) Cutoff finder: a comprehensive and straightforward Web application enabling rapid biomarker cutoff optimization. PLoS One 7(12):e51862

47. Lim JS, Sundar R, Chénard-Poirier M, Lopez J, Yap TA (2017) Emerging biomarkers for PD-1 pathway cancer therapy. Biomark Med 11(1):53–67

48. Yuasa T, Masuda H, Yamamoto S, Numao N, Yonese J (2017) Biomarkers to predict prognosis and response to checkpoint inhibitors. Int J Clin Oncol 22(4):629–634

49. Ji Z, Long H, Hu Y, Qiu X, Chen X, Li Z, Fan D, Ma B, Fan Q (2010) Expression of MDR1, HIF-1alpha and MRP1 in sacral chordoma and chordoma cell line CM-319. J Exp Clin Cancer Res 29:158

50. Li X, Ji Z, Ma Y, Qiu X, Fan Q, Ma B (2012) Expression of hypoxia-inducible factor-1alpha, vascular endothelial growth factor and matrix metalloproteinase-2 in sacral chordomas. Oncol Lett 3(6):1268–1274

51. Lee DH, Zhang Y, Kassam AB, Park MJ, Gardner P, Prevedello D, Henry S, Horbinski C, Beumer JH, Tawbi H, Williams BJ, Shaffrey ME, Egorin MJ, Abounader R, Park DM (2015) Combined PDGFR and HDAC inhibition overcomes PTEN disruption in chordoma. PLoS One 10(8):e0134426

52. Barsoum IB, Smallwood CA, Siemens DR, Graham CH (2014) A mechanism of hypoxia-mediated escape from adaptive immunity in cancer cells. Cancer Res 74(3):665–674

53. Noman MZ, Desantis G, Janji B, Hasmim M, Karray S, Dessen P, Bronte V, Chouaib S (2014) PD-L1 is a novel direct target of HIF-1alpha, and its blockade under hypoxia enhanced MDSC-mediated T cell activation. J Exp Med 211(5):781–790

54. Spranger S, Gajewski TF (2016) Tumor-intrinsic oncogene pathways mediating immune avoidance. Oncoimmunology 5(3):e1086862

55. Su Y, Ni Z, Wang G, Cui J, Wei C, Wang J, Yang Q, Xu Y, Li F (2012) Aberrant expression of microRNAs in gastric cancer and biological significance of miR-574-3p. Int Immunopharmacol 13(4):468–475

56. Tatarano S, Chiyomaru T, Kawakami K, Enokida H, Yoshino H, Hidaka H, Nohata N, Yamasaki T, Gotanda T, Tachiwada T, Seki N, Nakagawa M (2012) Novel oncogenic function of mesoderm development candidate 1 and its regulation by MiR-574-3p in bladder cancer cell lines. Int J Oncol 40(4):951–959

57. Chiyomaru T, Yamamura S, Fukuhara S, Hidaka H, Majid S, Saini S, Arora S, Deng G, Shahryari V, Chang I, Tanaka Y, Tabatabai ZL, Enokida H, Seki N, Nakagawa M, Dahiya R (2013) Genistein up-regulates tumor suppressor microRNA-574-3p in prostate cancer. PLoS One 8(3):e58929

58. Ujihira T, Ikeda K, Suzuki T, Yamaga R, Sato W, Horie-Inoue K, Shigekawa T, Osaki A, Saeki T, Okamoto K, Takeda S, Inoue S (2015) MicroRNA-574-3p, identified by microRNA library-based functional screening, modulates tamoxifen response in breast cancer. Sci Rep 5:7641

59. Zhao L, Yu H, Yi S, Peng X, Su P, Xiao Z, Liu R, Tang A, Li X, Liu F, Shen S (2016) The tumor suppressor miR-138-5p targets PD-L1 in colorectal cancer. Oncotarget 7(29):45370–45384

60. Fritzsching B, Fellenberg J, Moskovszky L, Sapi Z, Krenacs T, Machado I, Poeschl J, Lehner B, Szendroi M, Bosch AL, Bernd L, Csoka M, Mechtersheimer G, Ewerbeck V, Kinscherf R, Kunz P (2015) CD8+/FOXP3+-ratio in osteosarcoma microenvironment separates survivors from non-survivors: a multicenter validated retrospective study. Oncoimmunology 4(3):e990800

61. Asano Y, Kashiwagi S, Goto W, Kurata K, Noda S, Takashima T, Onoda N, Tanaka S, Ohsawa M, Hirakawa K (2016) Tumour-infiltrating CD8 to FOXP3 lymphocyte ratio in predicting treatment responses to neoadjuvant chemotherapy of aggressive breast cancer. Br J Surg 103(7):845–854

62. Roychoudhuri R, Eil RL, Restifo NP (2015) The interplay of effector and regulatory T cells in cancer. Curr Opin Immunol 33:101–111

63. Kim JR, Moon YJ, Kwon KS, Bae JS, Wagle S, Kim KM, Park HS, Lee H, Moon WS, Chung MJ, Kang MJ, Jang KY (2013) Tumor infiltrating PD1-positive lymphocytes and the expression of PD-L1 predict poor prognosis of soft tissue sarcomas. PLoS One 8(12):e82870

64. Kang MJ, Kim KM, Bae JS, Park HS, Lee H, Chung MJ, Moon WS, Lee DG, Jang KY (2013) Tumor-infiltrating PD1-positive lymphocytes and FoxP3-positive regulatory T cells predict distant metastatic relapse and survival of clear cell renal cell carcinoma. Transl Oncol 6(3):282–289

65. Zhao T, Li C, Wu Y, Li B, Zhang B (2017) Prognostic value of PD-L1 expression in tumor infiltrating immune cells in cancers: a meta-analysis. PLoS One 12(4):e0176822

66. Altman DG, Lausen B, Sauerbrei W, Schumacher M (1994) Dangers of using "optimal" cutpoints in the evaluation of prognostic factors. J Natl Cancer Inst 86(11):829–835

67. Mazumdar M, Glassman JR (2000) Categorizing a prognostic variable: review of methods, code for easy implementation and applications to decision-making about cancer treatments. Stat Med 19(1):113–132

68. Galon J, Costes A, Sanchez-Cabo F, Kirilovsky A, Mlecnik B, Lagorce-Pagès C, Tosolini M, Camus M, Berger A, Wind P, Zinzindohoué F, Bruneval P, Cugnenc PH, Trajanoski Z, Fridman WH, Pagès F (2006) Type, density, and location of immune cells within human colorectal tumors predict clinical outcome. Science 313(5795):1960–1964

69. Liu K, Yang K, Wu B, Chen H, Chen X, Chen X, Jiang L, Ye F, He D, Lu Z, Xue L, Zhang W, Li Q, Zhou Z, Mo X, Hu J (2015) Tumor-infiltrating immune cells are associated with prognosis of gastric cancer. Medicine (Baltimore) 94(39):e1631